Histol Histopathol (2019) 34: 745-753

http://www.hh.um.es

Histology and Histopathology

From Cell Biology to Tissue Engineering

The distribution and time-dependent expression of HIPK2 during the repair of contused skeletal muscle in mice

Miao Zhang[1,2,3]*, Meng-Zhou Zhang[1]*, Shu-Heng Wen[1], Ying-Fu Sun[1], Peng-Hao Jiang[1], Lin-Lin Wang[1,2,3], Rui Zhao[1,2,3], Chang-Liang Wang[1,2], Shu-Kun Jiang[1,2,3] and Da-Wei Guan[1,2,3]

[1]Department of Forensic Pathology, China Medical University School of Forensic Medicine, Liaoning Province, [2]Collaborative Laboratory of Intelligentized Forensic Science (CLIFS) and [3]Remote Forensic Consultation Center, Collaborative Innovation Center of Judicial Civilization, China University of Political Science and Law, Beijing, P.R. China

*These authors have contributed equally to this work

Summary. HIPK2 is an evolutionarily conserved serine/threonine kinase and is considered a co-regulator of an increasing number of transcription factors modulating a variety of cellular processes, including inflammation, proliferation and fibrosis. Skeletal muscle injuries repair is an overlapping event between inflammation and tissue repair. There are no reports about HIPK2 expression in skeletal muscles after trauma. A foundational study on distribution and time-dependent expression of HIPK2 was performed by immunohistochemical staining, Western blotting and quantitative real-time PCR, which is expected to obtain a preliminary insight into the functions of HIPK2 during the repair of contused skeletal muscle in mice. An animal model of skeletal muscle contusion was established in 50 C57B6/L male mice. Samples were taken at 1, 3, 5, 7, 9, 14, 17, 21 and 28 days after contusion, respectively (5 mice at each posttraumatic interval). 5 mice were employed as control. No HIPK2-positive staining was detected in uninjured skeletal muscle. Intensive immunoreactivties of HIPK2 were observed in polymorphonuclear cells, round-shaped mononuclear cells, regenerated multinucleated myotubes and spindle-shaped fibroblastic cells in the contused tissue. The HIPK2-positive cells were identified as neutrophils, macrophages and myofibroblasts by double immunofluorescent procedure. HIPK2 protein and mRNA expression were remarkably up-regulated after contusion by Western blotting and qPCR analysis. The results demonstrated that the expression of HIPK2 is distributed in certain cell types and is time-dependently expressed in skeletal muscle after contusion, which suggested that HIPK2 may participate in the whole process of skeletal muscle wound healing, including inflammatory response, muscle regeneration and fibrogenesis.

Key words: HIPK2, Skeletal muscle, Wound repair, Trauma

Offprint requests to: Shu-Kun Jiang or Da-Wei Guan, Department of Forensic Pathology, China Medical University School of Forensic Medicine, Liaoning Proviince, P.R. China. e-mail: skjiang@cmu.edu.cn or dwguan@cmu.edu.cn

DOI: 10.14670/HH-18-072

Introduction

Skeletal muscle injuries repair is a multi-factor regulated healing process and can be roughly divided into acute phase, repair phase and remodeling phase (Charge and Rudnicki, 2004). Within each phase, a myriad of orchestrated reactions and interactions between cells and chemicals are put into action. The whole process includes necrosis of the damaged muscle fibers, recruitment of inflammatory cells to phagocytose necrosis tissues and secrete inflammatory factors, activation of myogenic cells to differentiate and fuse into new myofibers as well as appearance of myofibroblasts to produce collagen fibers (Prisk and Huard, 2003).

Homeodomain-interacting protein kinases (HIPKs) family was first discovered as a binding partner of NK homeodomain transcription factors. It consists of four

members, defined by the presence of a highly homologous p38-MAPK-like kinase domain (Rinaldo et al., 2008). HIPK2, a member of HIPKs family, is an evolutionarily conserved serine/threonine kinase (Kim et al., 1998; Calzado et al., 2007) and is considered a co-regulator of an increasing number of transcription factors modulating a variety of cellular processes, including inflammation, proliferation and apoptosis (Calzado et al., 2007; Rinaldo et al., 2008; Poon et al., 2012). Recently, HIPK2 has also been identified as a master regulator in fibrogenesis. It was reported that knockout of HIPK2 attenuated kidney fibrosis in murine models of kidney fibrosis (Jin et al., 2012) and liver fibrosis in human HSC line (He et al., 2017).

Accumulated data showed that HIPK2 participates in modulating the process of inflammation, proliferation and fibrosis in several organs, while its spatiotemporal expression changes during the repair of contused skeletal muscle is still unknown. The aim of the study is to investigate the distribution and time-dependent expression of HIPK2 in contused skeletal muscle, which is expected to obtain a preliminary insight into the functions of HIPK2 during the repair of contused skeletal muscle in mice.

Materials and methods

Animal model of skeletal muscle contusion

All animal protocols were conformed to the 'Principles of Laboratory Animal Care' (National Institutes of Health publication no. 85-23, revised 1985) which seeks to minimize both the number of animals used in a procedure and any suffering that they might experience, and were performed according to the Guidelines for the Care and Use of Laboratory Animals of China Medical University. An animal model of muscle contusion was based on previously described studies (Kasemkijwattana et al., 1998; Wright-Carpenter et al., 2004; Xiao et al., 2016). Briefly, 50 healthy C57B6/L male mice (age, 8-10 weeks; weighing 18.1-23.1 g) were anesthetized with sodium pentobarbital (350 mg/kg) intraperitoneally. The right hindlimb was fixed on a board in a prone position by extending the knee and dorsiflexing the ankle to 90°. A 80 g (diameter, 12 mm) stainless steel ball was dropped from a height of 45 cm through a tube (interior diameter of tube, 14 mm) onto an impactor (Ota et al., 2011), resting with a surface of 28.26 mm^2 on the middle of the gastrocnemius muscle (GM) of the mice. Each mouse was individually housed in a cage and fed regular laboratory chow with water supplied ad libitum. A 12-hour day and night cycle was maintained. Mice were sacrificed by intraperitoneal injection of an overdose of sodium pentobarbital (350 mg/kg) at 1, 3, 5, 7, 9, 14, 17, 21 and 28 days after contusion (5 mice at each time point). Each muscle specimen was taken from wound site and equally divided into two blocks. One block was used for morphological evaluation, and another was used for molecular biological detection. No bone fracture was detected at dissection. For the 5 control mice, specimens were collected from the same site after anesthetization with an over-dose of pentobarbital.

Immunohistochemical staining and morphometric analysis

Fixed muscle specimens were embedded in paraffin. 5 μm-thick sections were prepared from paraffin-embedded tissue. Immunostaining was performed using the streptavidin-peroxidase method. The sections were deparaffinized in xylene, hydrated with a series of graded alcohol, and then heated in 0.01 mol/L sodium citrate buffer (pH 6.0) in a medical microwave oven for antigen retrieval. Subsequently, 3% hydrogen peroxide was applied for suppressing endogenous peroxidase activity. The sections were blocked with 10% non-immune goat serum to reduce non-specific binding. Then tissue sections were incubated with primary antibody. Rabbit anti-HIPK2 polyclonal antibody (dilution 1:200; PA5-40567, Invitrogen, CA, USA) overnight at 4°C, followed by incubation with Histostain-Plus kit according to the manufacturer's instructions (Zymed Laboratories, South San Francisco, CA, USA). The sections were routinely counterstained with hematoxylin. As immunohistochemical controls for immunostaining procedures, some sections were incubated with normal rabbit IgG, or phosphate buffered saline (PBS) in place of the primary antibodies. In addition, hematoxylin-eosin (H&E) staining was conventionally conducted.

Sections containing the largest contusion area were analyzed. HIPK2 positive cells were calculated under the 400-fold magnification in the contusion zones. All fields in the contusion zones were chosen for the calculations or evaluations in each section. All measurements and data analysis were performed independently by two pathologists in a blind manner. Morphometrical analysis was performed using Image-Pro Plus 6.0 (Media Cybernetics, Rockville, USA).

Cellular localization of HIPK2

Detection of HIPK2 in neutrophils, macrophages or myofibroblasts was conducted by double indirect immunofluorescent procedure. Briefly, deparaffinized sections were blocked with 5% BSA and incubated with rabbit anti-HIPK2 polyclonal antibody (dilution 1:50; PA5-40567, Invitrogen, CA, USA) at room temperature for 2 h. Thereafter, the sections were further incubated with Alexa Fluor® 555 donkey anti-rabbit IgG (dilution 1:200; A-31572, Invitrogen). Then, tissue sections were incubated with mouse anti-Neutrophil Marker (MPO) monoclonal antibody (dilution 1:50; ab90811, Abcam, Cambrideg, UK), rat anti-Macrophage Marker (F4/80) monoclonal antibody (dilution 1:50; ab6640, Abcam, Cambrideg, UK) or goat anti α-smooth muscle actin (α-SMA) polyclonal antibody (dilution 1:50; ab21027,

Abcam, Cambrideg, UK) overnight at 4°C. After incubation with Alexa Fluor® 488 donkey anti-mouse IgG (dilution 1:200; A-21202, Invitrogen), donkey anti-rat IgG (dilution 1:200; A-21208, Invitrogen) or donkey anti-goat IgG (dilution 1:200; A-11055, Invitrogen) at room temperature for 2 h, the nuclei were routinely counterstained with Hoechst 33258. The sections were mounted and observed under a fluorescence microscope. Normal rabbit, mouse, rat or goat IgG was used instead of primary antibodies as negative control.

For positive cell ratio evaluation, 10 microscopic fields were randomly selected at 400-fold magnification in the contused zones in each section, and the ratio of $HIPK2^+$ neutrophils, macrophages and myofibroblasts to the total number of cells in each positive cell type were calculated in each microscopic field. The average ratio of the 10 selected microscopic fields was evaluated in each wound specimen and expressed as percentage.

Protein extraction and immunoblotting assay

The skeletal muscle samples were ground into powder with liquid nitrogen using a grinder and homogenized with a sonicator in RIPA buffer (KGP9100, KeyGEN BioTECH, Nanjing, China) containing protease inhibitors and phosphatase inhibitors at 4°C. Homogenates were centrifuged at 12,000× g for 10 min three times at 4°C, and the resulting supernatants were collected. Protein concentrations were determined using the bicinchoninic acid method. Aliquots of the supernatants were diluted in an equal volume of 6x electrophoresis sample buffer and boiled for 5min. Protein lysates (30 μg) were separated on a 12% sodium dodecyl sulfate-poly-acrylamide electrophoresis gel and transferred onto polyvinylidene fluoride membranes (Millipore, Billerica, MA, USA). After being blocked with 5% BSA in Tris-buffered saline with Tween-20 at room temperature for 2h, the blots were incubated with rabbit anti-HIPK2 polyclonal antibody (dilution 1:400; PA5-40567, Invitrogen, CA, USA) or rabbit anti-GAPDH polyclonal antibody (dilution 1:2500; ab9485, Abcam, Cambridge, UK) at 4°C overnight and horseradish peroxidase conjugated goat anti-rabbit IgG (sc-2004, Santa Cruz Biotechnology, CA, USA) at 1:2,000 dilution at room temperature for 2h. The blotting was visualized with Western blotting luminol reagent (sc-2048, Santa Cruz Biotechnology, CA, USA) and by the Electrophoresis Gel Imaging Analysis System (MF-ChemiBIS 3.2, DNR Bio-Imaging Systems, ISR). Subsequently, densito-metric analyses of the bands were semiquantitatively conducted using Scion Image software (Scion Corporation, MD, USA).

Total RNA extraction and quantitative real-time PCR analysis

Total RNA was isolated from the skeletal muscle specimens with RNAiso Plus (9108, Takara Biotechnology, Shiga, Japan) according to the manufacturer's instructions. OD values of each RNA sample were measured by ultraviolet spectrophotometer. A260/A280 ranged from 1.8 to 2.0. Then, the RNA (250 ng) was reversetranscribed into cDNA using the PrimeScript™ RT reagent Kit (RR047A, Takara Biotechnology, Shiga, Japan). The resulting cDNA was used for quantitative real-time PCR with the sequence-specific primer pairs for HIPK2 and GAPDH (Table 1; Takara Biotechnology, Shiga, Japan). Quantitative real-time PCR amplification was performed by ABI 7500 Real-Time PCR System (Applied Biosystems, Foster City, CA) using SYBR® PrimeScript™ RT-PCR Kit (RR820A, Takara Biotechnology, Shiga, Japan) followed by the parameters: 2 μl cDNA was loaded to each quantitative real-time PCR reaction. A denaturing step was at 95°C for 30 s followed by 15 s at 95°C, 34 s at 60°C, 15 s at 95°C, 60 s at 60°C, 15 s at 95°C for 40 cycles. PCR-generated fragments for HIPK2 and GAPDH primer sets were 21 and 22 bp, respectively. Dissociation curve analysis of PCR products revealed single peaks, indicating specific amplification products. The relative expression level of HIPK2 was normalized by subtracting the corresponding GAPDH threshold cycle (CT) values using the $\Delta\Delta C_T$ comparative method (Schmittgen et al., 2000).

Statistical analysis

Results were expressed as mean ± standard deviation (SD) or ratio, and statistical significance was determined by one-way ANOVA followed by Tukey's multiple comparisons test, Fisher's exact test or Mann Whitney U test using PRISM 6.0 software (GraphPad Software, Inc.). Data were considered significantly different for $P<0.05$.

Table 1. qPCR primer sequences.

Gene	Species	Primer		GenBank ID
HIPK2	Mus	Forward Reverse	TGTTGGTAGAATGTGACAGCC GAGGACTTGGACTTGAAGGAG	NM_010433
GAPDH	Mus	Forward Reverse	CTTTGTCAAGCTCATTTCCTGG TCTTGCTCAGTGTCCTTGC	NM_008084

Results

Histological examination

In sections stained with H&E, hemorrhage, edema and necrosis were observed in the contused skeletal muscles. A great number of polymorphonuclear cells (PMNs) appeared in wound zones at 1 day post-injury (Fig. 1b). Round-shaped mononuclear cells (MNCs) appeared in wound zones at 1 day, which remarkably increased in number at 3 days post-injury. Besides, spindle-shaped fibroblastic cells (FBCs) appeared in the wound zones at 3 days post-injury (Fig. 1c). From 5 to 14 days post-injury, a large number of FBCs, concomitant with regenerated multinucleated myotubes were observed in the wound zones (Fig. 1d-g). From 14 to 28 days post-wounding, FBCs and fibrotic tissue were still observed in the wounds (Fig. 1h).

Immunohistochemical and double indirect immunofluorescence analyses

In the control skeletal muscle specimens, no HIPK2-positive staining was detected in uninjured skeletal muscle (Fig. 2a). In the injured skeletal muscle samples, most PMNs showed HIPK2-positive at 1 day post-injury (Fig. 2b). A great number of MNCs and FBCs were positively immunostained with anti-HIPK2 antibody at 3 days post-injury (Fig. 2c). From 5 to 14 days post-injury, HIPK2 immunoreactivity was mainly detected in FBCs and regenerated multinucleated myotubes (Fig. 2d-g). From 14 to 28 days post-injury, there were still FBCs labeled with anti-HIPK2 antibody in the fibrotic tissue (Fig. 2g,h). Furthermore, the number of $HIPK2^+$ cells and the average ratio of $HIPK2^+$ cells to the total number of cells were calculated in each microscopic field. With time extension of post-traumatic interval, the number and the ratio of $HIPK2^+$ cells gradually increased from 1 day post-injury and peaked at 7 days post-injury. Thereafter, they gradually decreased until 28 days post-injury (Fig. 2i,j).

For the identification of PMNs, MNCs and FBCs, co-localization of HIPK2 with MPO (neutrophil marker), F4/80 (macrophage marker) and α-SMA (myofibroblast marker) were conducted. At 1 day post-injury, a great number of PMNs infiltrated into the injured zones showed $HIPK2^+/MPO^+$ (Fig. 3a-d). After 1 day post-injury, the $HIPK2^+/MPO^+$ double-positive cells decreased in number at the wound zones. At 3 days post-injury, a large number of MNCs infiltrated into the injured sites showed $HIPK2^+/F4/80^+$ (Fig. 3e-h). From 5 days post-injury, fewer $HIPK2^+/F4/80^+$ cells could be detected in the wound zones. With time extension of post-traumatic interval, FBCs infiltrated into the injured sites showed $HIPK2^+/\alpha\text{-}SMA^+$ (Fig. 3i-l) from 3 days post-injury and peaked at 7 days post-injury. After that, $HIPK2^+/\alpha\text{-}SMA^+$ cells decreased in number gradually.

Besides, the average ratios of $HIPK2^+/MPO^+$, $HIPK2^+/F4/80^+$, and $HIPK2^+/\alpha\text{-}SMA^+$ positive cells to the total number of cells in each positive cell type were calculated in each microscopic field. The average ratio of $HIPK2^+/MPO^+$ peaked at 1 day post-injury, and then it gradually reduced in number until 5 days post-injury. The average ratios of $HIPK2^+/F4/80^+$ and $HIPK2^+/\alpha\text{-}SMA^+$ positive cells generally up-regulated from 1 and 3 days post-injury and maximized at 5 and 7 days post-injury, respectively. And then, they gradually reduced in number until 28 days post-injury, respectively (Fig. 3m).

Western blotting and qPCR

The expression of HIPK2 protein could not be detected in normal muscles but was detected in injured skeletal muscle specimens. Its expression was gradually up-regulated within 7 days after contusion and down-regulated thereafter, which maximized at 7 days by semi-quantitative analysis. There were significant differences in the relative intensity of HIPK2 to GAPDH between 3, 5, 7, 9 and 14 days as compared with their preceding groups (Fig. 4a,b).

Relative quantity of HIPK2 mRNA expression in mice skeletal muscle was also assayed by qPCR throughout the 28 days after contusion. The mRNA expression was generally up-regulated within 7 days post-injury and down-regulated thereafter. The trend was consistent with changes in protein expression. Significant differences could be observed between control group and 3, 5, 7, 9, and 14 days post-injury (Fig. 4c).

Discussion

Skeletal muscle wound healing is a highly orchestrated process, which consists of four phases including necrosis of the damaged muscle fibers, recruitment of inflammatory cells, activation of myogenic cells to differentiate and fuse into new myofibers as well as appearance of myofibroblasts to form fibrotic lesion (Prisk and Huard, 2003; Charge and Rudnicki, 2004). Our present study confirmed the similar findings on morphological changes.

HIPK2 is considered to be a tumor suppressor. However, a previous study had reported that HIPK2 modulates inflammatory response. HIPK2 over-expression reduced oxidative stress and the levels of inflammatory cytokines (Li et al., 2018). Overexpression of WT-HIPK2 in HIV-infected renal tubular epithelial cells enhanced the expression of NF-κB targeted genes, while overexpression of kinase dead (KD)-HIPK2 suppressed NF-κB activation and inhibited the expression of its downstream target genes (Nugent et al., 2015). In the present study, we observed that HIPK2 was expressed in neutrophils and macrophages, and the average ratios of HIPK2-positive neutrophils and macrophages peaked at 1 and 5 days post-injury. Besides, the HIPK2 protein and mRNA expression were up-regulated at inflammatory phase in skeletal muscles after contusion. These results indicated that HIPK2 may

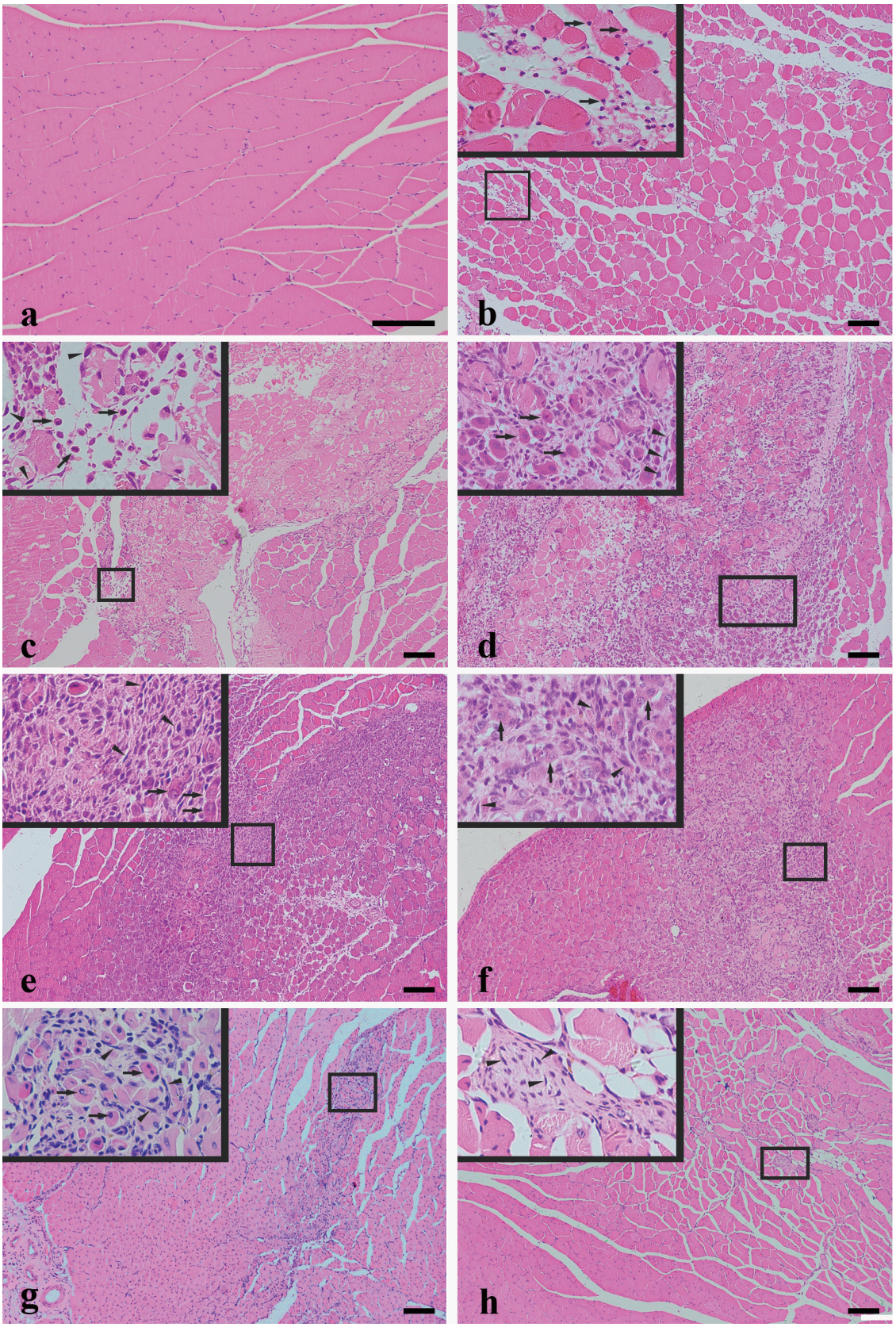

Fig. 1. H&E staining in mice skeletal muscle after contusion. **a.** The morphology of normal skeletal muscles as a control. **b.** Polymorphonuclear cells (PMNs) are detected at 1 day after contusion (arrows). **c.** Round-shaped mononuclear cells (MNCs, arrows) and spindle-shaped fibroblastic cells (FBCs, arrowheads) are present in the injured areas at 3 days after contusion. **d, e, f, g.** Regenerated multinucleated myotubes (arrows) and FBCs (arrowheads) are present in the injured areas at 5, 7, 9 and 14 days after contusion, respectively. **h.** Spindle-shaped FBCs (arrowheads) and fibrotic tissue are still seen in the wound zone at 28 days after contusion. Scale bar: 100 μm.

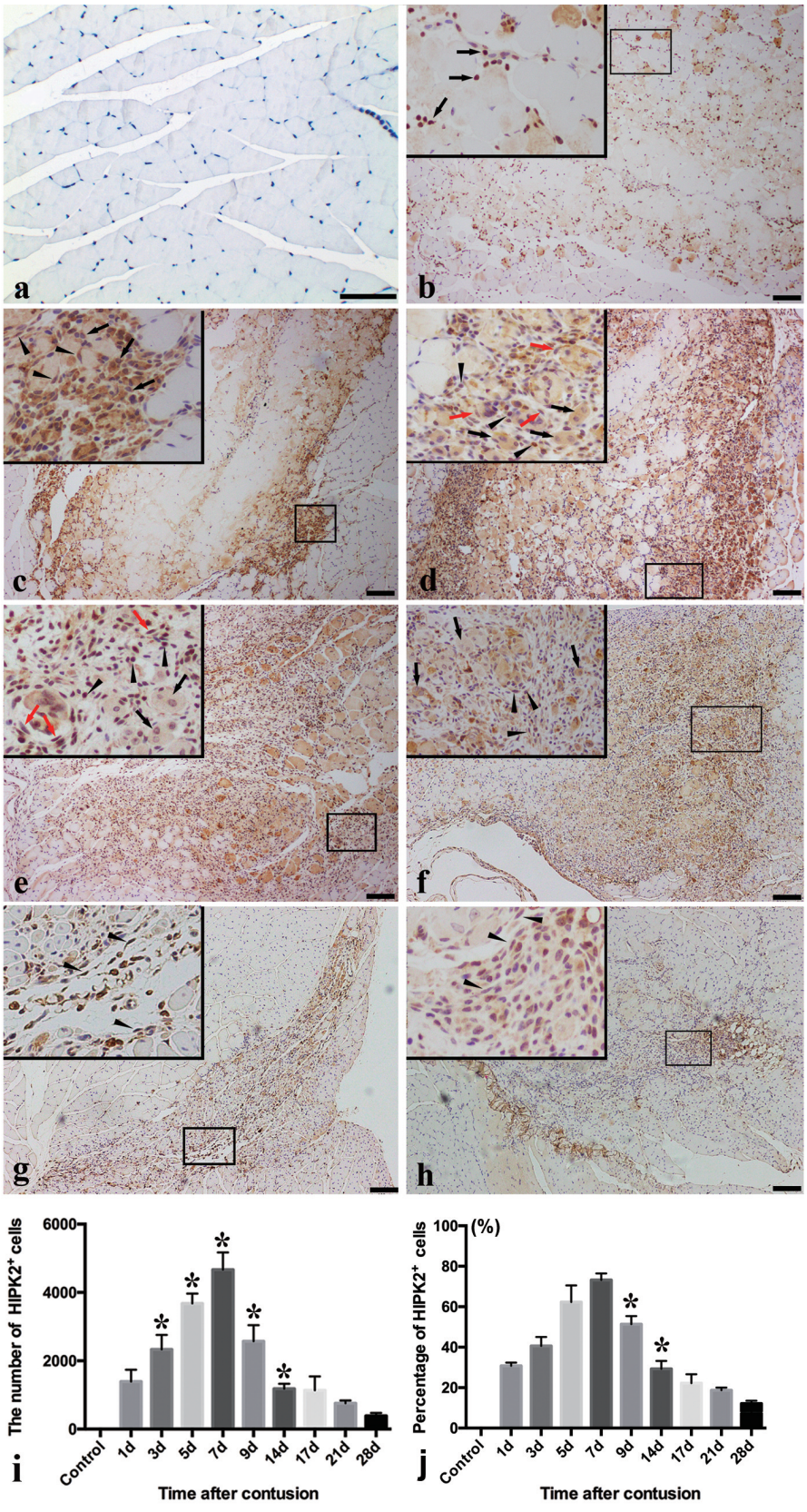

Fig. 2. Immunohistochemical staining of HIPK2 in the wound zones of skeletal muscle contusion. **a.** HIPK2-positive staining could not be detected in uninjured skeletal muscle. **b.** HIPK2-positive staining is observed in PMNs (arrows) at 1 day after contusion. **c.** HIPK2-positive staining is observed in MNCs (arrows) and FBCs (arrowheads) at 3 days after contusion. **d, e.** HIPK2-positive staining is observed in regenerated multinucleated myotubes (black arrows), MNCs (black arrowheads) and FBCs (red arrows) at 5 and 7 days after contusion, respectively. **f.** HIPK2-positive staining is observed in regenerated multinucleated myotubes (arrows) and FBCs (arrowheads) at 9 days after contusion. **g, h.** HIPK2-positive staining is observed in FBCs (arrowheads) in the injured areas at 14 and 28 days after contusion. **i.** The number of HIPK2+ cells in the contusion zones in relation to wound age. The number of HIPK2+ cells peaked at 7 days post-injury. Data were presented as mean ± SD and analyzed using one-way ANOVA followed by Tukey's multiple comparisons test. *: $P<0.05$ (vs preceding posttraumatic group). **j.** The average ratio of HIPK2+ cells to the total number of cells were calculated in each microscopic field. The average ratio of HIPK2+ cells peaked at 7 days post-injury. Data were presented as ratio and analyzed using Fisher's exact test. *: $P<0.05$ (vs preceding posttraumatic group). Scale bar: 100 μm.

be involved in inflammatory response during skeletal muscle wound healing in mice.

Muscle regeneration is a critical event for functional recovery of injured skeletal muscles (Filippin et al., 2011) and it is closely associated with macrophages. During the process of skeletal muscle wound healing, macrophages are required for triggering the earliest events by activating quiescent satellite cells (Lescaudron et al., 1999). And the activated satellite cells proliferate and differentiate into myoblasts. The newly formed myoblasts fuse with each other to form multinucleated myofibers (Jarvinen et al., 2005). Besides, a previous study reported that HIPK2 determines the threshold and kinetics of gene expression in proliferating myoblasts and during the initial steps of myogenesis in murine C2C12 cells (de la Vega et al., 2013). In our present

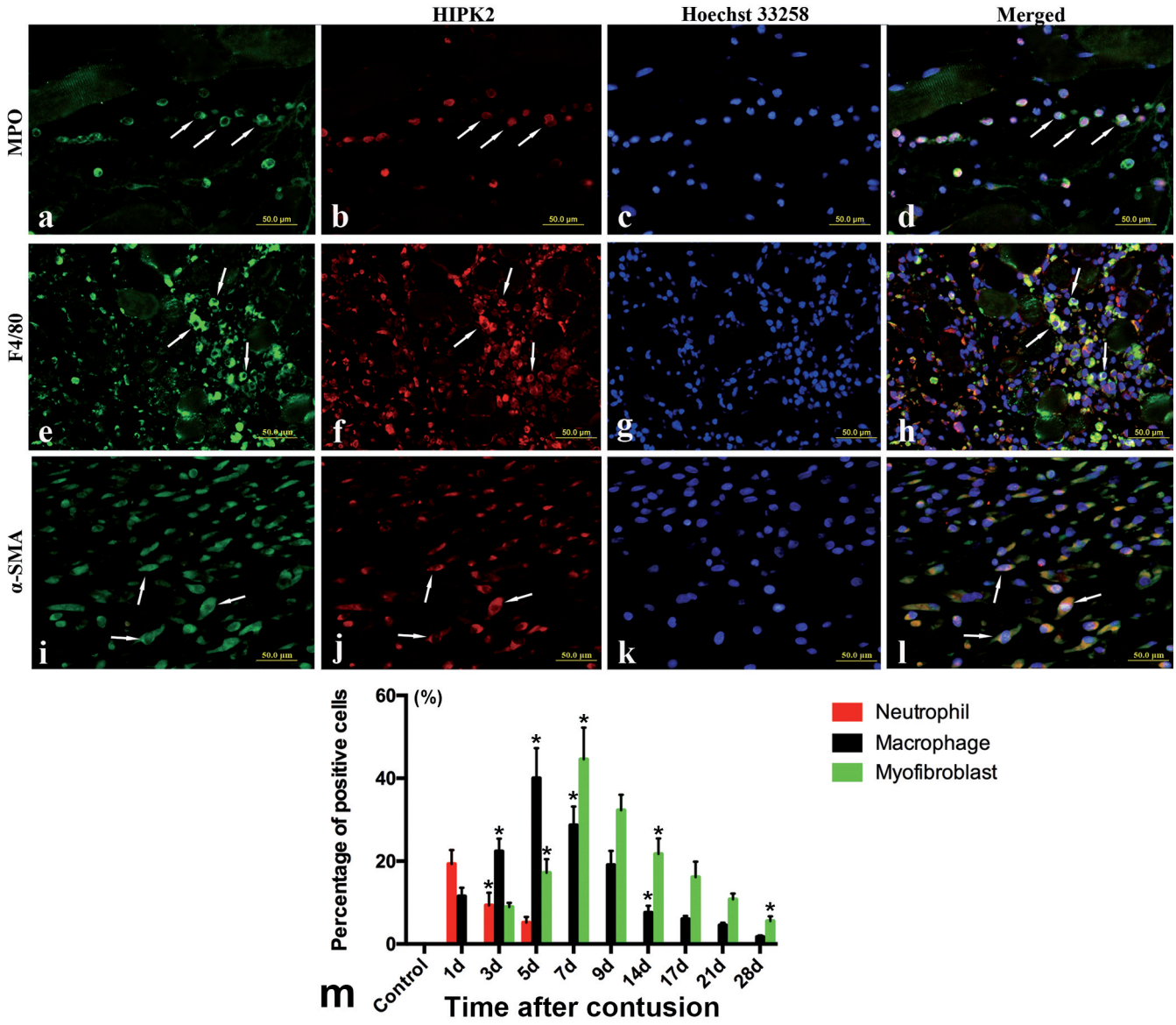

Fig. 3. Double immunofluorescent staining was performed for identifying HIPK2-expressing cells after contusion. **a, e, i.** The sample was immunostained with anti-MPO, F4/80 and α-SMA (green) at 1, 3 and 14 days, respectively. **b, f, j.** The sample was immunostained with anti-HIPK2 (red). **d, h, l.** Signals were digitally merged. The HIPK2$^+$/MPO$^+$, HIPK2$^+$/F4/80$^+$ and HIPK2$^+$/α-SMA$^+$ cells are presented as yellow signal in the merged image. Representative results from at least 3 individual experiments are shown. Scale bar: 50 μm. **m.** The average ratios of HIPK2-positive neutrophils, macrophages and myofibroblasts to the total number of cells in each positive cell type were calculated in each microscopic field. The average ratios of HIPK2-positive neutrophils, macrophages and myofibroblasts peaked at 1, 5 and 7 days post-injury, respectively. Data were presented as ratio and analyzed using Fisher's exact test. *: $P<0.05$ (vs preceding posttraumatic group).

study, both macrophages and regenerated multinucleated myotubes expressed HIPK2 in the contused zones, which indicated that HIPK2 may also be involved in regulating skeletal muscle regeneration in mice.

Fibrosis is an inevitable consequence of wound repair in many organs and tissues. And the repair of skeletal muscle injuries is typically an overlapping event between inflammation and tissue repair. Macrophages promote fibroblast activation and proliferation by stimulating IL-1β, TGF-β and other cytokines (Barron and Wynn, 2011). Meanwhile, fibroblasts summon and stimulate macrophages by producing MCP-1 and other chemokines (Seki et al., 2007; Friedman, 2008). Myofibroblasts, which are characterized by a contractile phenotype and the presence of α-SMA stress fibers, play an important role in collagen synthesis and fibrosis (Lotersztajn et al., 2005). It was found that fibroblasts and myofibroblasts produced similar types of procollagens, namely collagens I and III, in similar proportions at or near a 1:1 ratio.

However, myofibroblasts at early passage produced threefold more procollagens than did fibroblasts at the same stage of passage, while similar quantities were produced in each at late passage (Oda et al., 1990). A previous study reported that HIPK2 is closely associated with fibrogenesis in certain tissues such as the liver, lung and kidney. And knockdown of HIPK2 attenuated the activation of myofibroblast by inhibiting the TGF-β1/Smad3 signaling pathway (Ricci et al., 2013; Fan et al., 2014; Nugent et al., 2015; He et al., 2017). In this study, we observed that HIPK2-positive macrophages and myofibroblast come to appear as early as 3 days post-injury, which indicated that HIPK2 participates in modulating the functions of macrophages and fibroblasts in the early stage of inflammation phase. Furthermore, we also observed a large number of HIPK2-positive myofibroblasts in the fibrosis phase. Therefore, we speculate that HIPK2 also participates in modulating fibrogenesis during skeletal muscle wound healing in mice.

In conclusion, we first demonstrate that HIPK2 is dynamically distributed in neutrophils, macrophages, regenerated multinucleated myotubes and myofibroblasts and time-dependently expressed during the repair of skeletal muscle contusion, which indicated that HIPK2 may participate in the whole process of skeletal muscle wound healing, including inflammatory response, muscle regeneration and fibrogenesis. Furthermore, HIPK2 may be a new target for the treatment of skeletal muscle injury.

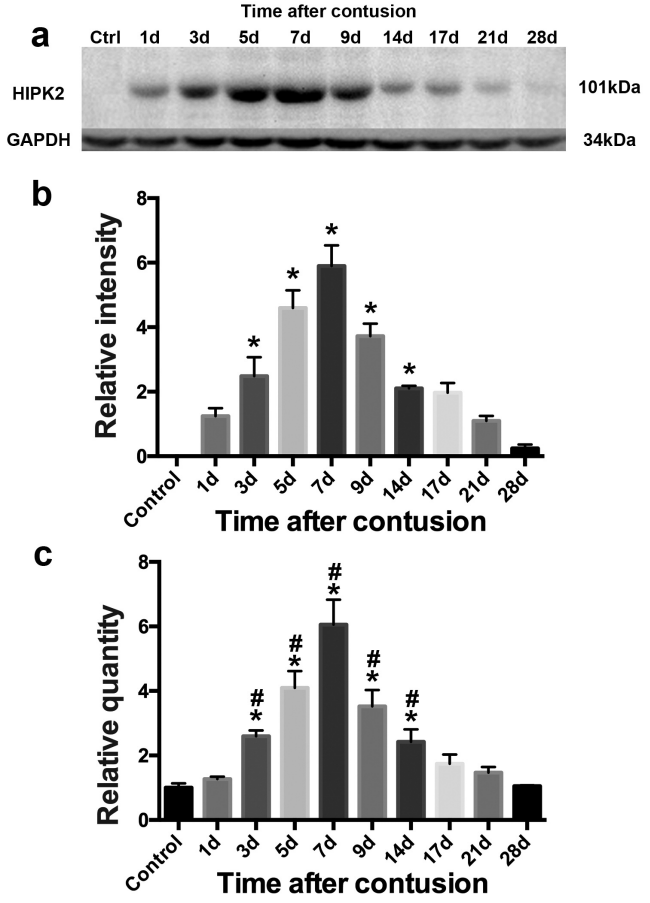

Fig. 4. a. Analysis of HIPK2 and GAPDH protein from skeletal muscle specimens by Western blotting. Representative results from 5 individual animals are shown. **b.** Relative intensity of HIPK2 to GAPDH. There were significant differences in the relative intensity of HIPK2 to GAPDH between 3, 5, 7, 9 and 14 days as compared with their preceding groups. **c.** Analysis of HIPK2 and GAPDH mRNA expression from skeletal muscle specimens by qPCR. Significant differences could be observed between control group and 3, 5, 7, 9, and 14 days post-injury. Data for Western blotting were presented as mean ± SD and analyzed using one-way ANOVA followed by Tukey's multiple comparisons test. qPCR data were presented as mean ± SD and analyzed using Mann Whitney U test. *: P<0.05 (vs preceding posttraumatic group); #: P<0.05 (vs control group).

Acknowledgements. This study was financially supported in part by grants from research fund for New Teachers Program by China Medical University (XZR20160034) and from projects funded by National Natural Science Foundation of China (81671862, 81772023 and 81871529).

References

Barron L. and Wynn T.A. (2011). Fibrosis is regulated by th2 and th17 responses and by dynamic interactions between fibroblasts and macrophages. Am. J. Physiol. Gastrointest. Liver Physiol. 300, G723-728.

Calzado M.A., Renner F., Roscic A. and Schmitz M.L. (2007). HIPK2: A versatile switchboard regulating the transcription machinery and cell death. Cell Cycle 6, 139-143.

Charge S.B. and Rudnicki M.A. (2004). Cellular and molecular regulation of muscle regeneration. Physiol. Rev. 84, 209-238.

de la Vega L., Hornung J., Kremmer E., Milanovic M. and Schmitz M.L. (2013). Homeodomain-interacting protein kinase 2-dependent repression of myogenic differentiation is relieved by its caspase-

mediated cleavage. Nucleic Acids Res. 41, 5731-5745.

Fan Y., Wang N., Chuang P. and He J.C. (2014). Role of HIPK2 in kidney fibrosis. Kidney Int. Suppl. 4, 97-101.

Filippin L.I., Cuevas M.J., Lima E., Marroni N.P., Gonzalez-Gallego J. and Xavier R.M. (2011). Nitric oxide regulates the repair of injured skeletal muscle. Nitric Oxide 24, 43-49.

Friedman S.L. (2008). Hepatic stellate cells: Protean, multifunctional, and enigmatic cells of the liver. Physiol. Rev. 88, 125-172.

He P., Yu Z.J., Sun C.Y., Jiao S.J. and Jiang H.Q. (2017). Knockdown of HIPK2 attenuates the pro-fibrogenic response of hepatic stellate cells induced by TGF-beta1. Biomed. Pharmacother. 85, 575-581.

Jarvinen T.A., Jarvinen T.L., Kaariainen M., Kalimo H. and Jarvinen M. (2005). Muscle injuries: Biology and treatment. Am. J. Sports Med. 33, 745-764.

Jin Y., Ratnam K., Chuang P.Y., Fan Y., Zhong Y., Dai Y., Mazloom A.R., Chen E.Y., D'Agati V., Xiong H., Ross M.J., Chen N., Ma'ayan A. and He J.C. (2012). A systems approach identifies hipk2 as a key regulator of kidney fibrosis. Nat. Med. 18, 580-588.

Kasemkijwattana C., Menetrey J., Somogyl G., Moreland M.S., Fu F.H., Buranapanitkit B., Watkins S.C. and Huard J. (1998). Development of approaches to improve the healing following muscle contusion. Cell Transplant. 7, 585-598.

Kim Y.H., Choi C.Y., Lee S.J., Conti M.A. and Kim Y. (1998). Homeodomain-interacting protein kinases, a novel family of co-repressors for homeodomain transcription factors. J. Biol. Chem. 273, 25875-25879.

Lescaudron L., Peltekian E., Fontaine-Perus J., Paulin D., Zampieri M., Garcia L. and Parrish E. (1999). Blood borne macrophages are essential for the triggering of muscle regeneration following muscle transplant. Neuromuscul. Disord. 9, 72-80.

Li R., Shang J., Zhou W., Jiang L., Xie D. and Tu G. (2018). Overexpression of HIPK2 attenuates spinal cord injury in rats by modulating apoptosis, oxidative stress, and inflammation. Biomed. Pharmacother. 103, 127-134.

Lotersztajn S., Julien B., Teixeira-Clerc F., Grenard P. and Mallat A. (2005). Hepatic fibrosis: Molecular mechanisms and drug targets. Annu. Rev. Pharmacol. Toxicol. 45, 605-628.

Nugent M.M., Lee K. and He J.C. (2015). HIPK2 is a new drug target for anti-fibrosis therapy in kidney disease. Front. Physiol. 6, 132.

Oda D., Gown A.M., Vande Berg J.S. and Stern R. (1990). Instability of the myofibroblast phenotype in culture. Exp. Mol. Pathol. 52, 221-234.

Ota S., Uehara K., Nozaki M., Kobayashi T., Terada S., Tobita K., Fu F.H. and Huard J. (2011). Intramuscular transplantation of muscle-derived stem cells accelerates skeletal muscle healing after contusion injury via enhancement of angiogenesis. Am. J. Sports Med. 39, 1912-1922.

Poon C.L., Zhang X., Lin J.I., Manning S.A. and Harvey K.F. (2012). Homeodomain-interacting protein kinase regulates hippo pathway-dependent tissue growth. Curr. Biol. 22, 1587-1594.

Prisk V. and Huard J. (2003). Muscle injuries and repair: The role of prostaglandins and inflammation. Histol. Histopathol. 18, 1243-1256.

Ricci A., Cherubini E., Ulivieri A., Lavra L., Sciacchitano S., Scozzi D., Mancini R., Ciliberto G., Bartolazzi A., Bruno P., Graziano P. and Mariotta S. (2013). Homeodomain-interacting protein kinase2 in human idiopathic pulmonary fibrosis. J. Cell Physiol. 228, 235-241.

Rinaldo C., Siepi F., Prodosmo A. and Soddu S. (2008). HIPKs: Jack of all trades in basic nuclear activities. Biochim. Biophys. Acta 1783, 2124-2129.

Schmittgen T.D., Zakrajsek B.A., Mills A.G., Gorn V., Singer M.J. and Reed M.W. (2000). Quantitative reverse transcription-polymerase chain reaction to study mrna decay: Comparison of endpoint and real-time methods. Anal. Biochem. 285, 194-204.

Seki E., De Minicis S., Osterreicher C.H., Kluwe J., Osawa Y., Brenner D.A. and Schwabe R.F. (2007). Tlr4 enhances tgf-beta signaling and hepatic fibrosis. Nat. Med. 13, 1324-1332.

Wright-Carpenter T., Opolon P., Appell H.J., Meijer H., Wehling P. and Mir L.M. (2004). Treatment of muscle injuries by local administration of autologous conditioned serum: Animal experiments using a muscle contusion model. Int. J. Sports Med. 25, 582-587.

Xiao W., Liu Y. and Chen P. (2016). Macrophage depletion impairs skeletal muscle regeneration: The roles of pro-fibrotic factors, inflammation, and oxidative stress. Inflammation 39, 2016-2028.

Accepted December 5, 2018